We are IntechOpen, the world's leading publisher of Open Access books Built by scientists, for scientists

6,900
Open access books available

185,000
International authors and editors

200M
Downloads

Our authors are among the

154
Countries delivered to

TOP 1%
most cited scientists

12.2%
Contributors from top 500 universities

WEB OF SCIENCE™

Selection of our books indexed in the Book Citation Index in Web of Science™ Core Collection (BKCI)

Interested in publishing with us?
Contact book.department@intechopen.com

Numbers displayed above are based on latest data collected.
For more information visit www.intechopen.com

19

Dye Doped Polymer-Filled Nanoporous Glass – a New Class of Materials for Laser Optics

Modest Koldunov and Alexander Manenkov
A.M.Prokhrov General Physics Institute, Russian Academy of Sciences, Moscow Russia

1. Introduction

A subject of this chapter is a dye-activated polymer-filled nanoporous glass as a new composite material for laser optics. It has been realized for the first time in 1988 [1] as a Q-switching optical element for lasers. Motivation for that work was to improve properties of Q-switchers based on dye-activated balk polymers possessing good optical properties, but having rather poor thermo-optical and mechanical properties, which lead to thermo-optical distortions of laser beams and to a mechanical deformation of an element surface at variations of temperature and humidity of an environment. To reduce these negative effects of the optical polymer an idea was proposed to insert the polymer element into a rigid cage. This idea has been realized at first in a triplex element: a polymer film clamped between glass plates. Another approach to solving the problem was synthesizing a polymer in pores of nonporous glass (NPG), i.e. making a polymer-filled nanoporous glass (PFNPG) composite

Note that a technology of NPG has been well developed by that time [2-4]. Mention also that attempts to make NPG-based laser elements were performed: laser operation, Q-switching, and mode-locking have been demonstrated in porous glass elements impregnated with liquid dye solutions [5-7].

Difficulty of making the composite NPG-polymer is connected, mainly, with peculiarity of a polymerization process in pores. A significant shrinkage effect takes place at polymerization that can create porous leading to light scattering. This problem has been solved in [1] and a technology of the PFNPG composite of high optical quality has been developed.-

Comprehensive studies [8-25] of properties of PFNPG composite elements made by the developed technology confirmed that the composite has a significant advantage over the bulk polymer. The composite preserving positive properties of modified optical polymers (high solubility of organic dyes, high laser-induced damage resistance) exclude its negative properties (poor thermo-optical quality, sensitivity to temperature and humidity variations).

A goal of this chapter is analyzing the PFNPG composite as the laser optical material. The chapter consists of four sections.

In the first section general requirements to laser optics elements are briefly discussed.

In the second section principles of the PFNPG composite technology are described.

In the third section the results of comprehensive studies of the composite properties are reported and analyzed.

In the forth section experimental results of studies of PFNPG laser elements doped with different type functional organic compounds are presented and discussed.

2. Requirements to laser optical elements: a general analysis

Before a detailed analysis of properties of the dye-impregnate polymer-filled nanoporous glass it is reasonable to considerer qualitatively, in a general form, the most important characteristics of laser optics materials. General properties, to which the laser optics materials for laser optics applications have to be satisfied, are as follows.

- Transparency in an operation wavelength range, due to both light absorption and scattering loses, has to be high.
- Mechanical strength has to be high enough for a treatment of the optical elements using a standard glass fabrication technology.
- Laser-induced damage resistance of the materials in both the single-shot (1×1) and multi-shot (1×N) irradiation regimes has to be high.
- Thermo-optical figure of merit of the material, characterized by the parameter $\mu = \chi(dn/dT)^{-1}$, where χ is thermal conductivity, n is refractive index, T is temperature, has to be high enough to avoid optical distortions of a propagating radiation in high-power laser systems operating, especially, at high repetition rates.
- Functional organic compounds impregnated to a host material to get a desirable optical effect, active-laser emission or passive-radiation control, i.e. Q-switching and mode-locking, have to be distributed inside the material homogeneously to avoid, for example, luminescence quenching in lasing elements.

Speaking about the material characteristics, note that measurements of absolute values of some of them are significant problems. On this reason properties of the PFNPG composite, reported in this chapter, were investigated in comparison with the same properties of the bulk modified polymethylmathacrilate (MPMMA) fabricated from the same monomer composition as the polymer component of the composite. For comparison, in Table 1 some characteristics of PFNPG and MPMMA [19,26] are presented.

	Bulk Polymer	PFNPG-composite
Solubility of dyes, mol/l	~ 10^{-2}	~ 10^{-2}
Optical transparency range, nm	300÷1600	300÷1600
Light scattering	Very weak	Weak
Thermo-optical Figure of Merit*, W/m	~ 10^3	~ 10^5
Laser-induced Damage Resistance**, 1×1, J/cm^2	~ 60	~ 70
Laser-induced Damage Resistance**, 1×200, J/cm^2	~ 5	~ 30
Micro-hardness, N/mm^2	~ 100	~ 2000
Climatic resistance	Low	High

* Thermo-optical Figure of Merit $\mu = \chi(dn/dT)^{-1}$, χ : thermal conductivity, n: refractive index, T : temperature.

** At pulsewidth 10 ns, wavelength 1064 nm. 1×1: single-shot regime, 1×200: multi-shot regime

Table 1.

The data, presented in Table 1, confirm the statement in the introduction above that the PFNPG composite has significantly better properties than those of the bulk polymer.

3. Technology of PFNPG-composite

3.1 Structure of NPG

Studies of porous glasses have been started in 1930th [2-4]. Technology of their fabrication is based on a liquation phenomenon consisting of the following.

Some of the multi-component glasses (for example, $SiO_2 \times B_2O_3 \times Na_2O \times R_2O_3$) at a thermal treatment (typically, at 550-600° C) are segregated into chemically different phases: a resistant silicate SiO_2 – enriched phase and a non-resistant sodium-borate phase containing, mostly, Na_2O and B_2O_3. It is important that the two phase segregation may be different depending on a relative content of the components: one phase can be distributed in the other phase (in a droplet form) constituting a "colloidal solution" or both phases can form a two interpenetrating set ("two-cage" structure).

The nanoporous glass is fabricated from compositions which form, in the segregation process, two interpenetrating nets. The example of such the composition is 59.0 $SiO_2 \times 33.2B_2O_3 \times 4.0Na_2O \times 3.8$ K_2O. For obtaining the nanoporous glass the chemically unstable sodium-borate phase is removed by acid pickling. Porous glasses obtained by this technology content, typically, 93÷99% SiO_2, 2÷5% B_2O_3, 0.05÷0.5% NO_2 and K_2O.

This technology includes the thermal treatment, acid treatment, water washing, and drying. Porosity of the NPG defined as $P = V_p / V_g$, the ratio of total pores volume V_p to a glass volume V_g, and the porous size distribution are important characteristics for the PFNPG composite material intended for optical applications. The value of P depends on the initial content of the glass and the technology of its treatment. Typically, P=45%. Measurement of the pore size-distribution is based on investigation of an isothermal water vapor absorption in NPG (water porometery method [27]). Results of such the measurements show that the pore size distribution in NPG samples fabricated by the technology, described above, is narrow, single-modal. The typical example is shown in Fig 1.

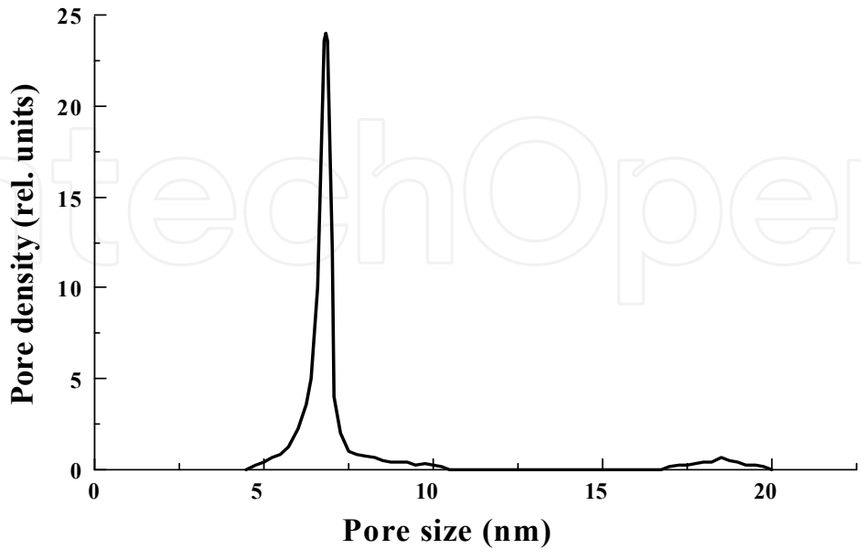

Fig. 1. Pore size distribution in NPG obtained with the water porometery method. The initial glass composition is $59{,}0SiO_2 \times 33{,}2B_2O_3 \times 4{,}0Na_2O \times 3{,}8K_2O$. (After Ref. [12])

Varying a content of the initial glass and a thermotreatment regime one can get the nanoporous glasses with pore sizes in the range of 1÷2000 nm. However, for optical applications the pore sizes not exceeding 20 nm are of the most interest.
Note that the water porometery method can not give information on a structure of the NPG. The more detailed information is obtained with electron microscopy. Application of this technique has shown that pores in NPG contain some amount of small silicate particles [28]. This type of particles is seen in Fig. 1 (weak peak at 18 nm).

3.2 Content and making technology of PFNPG

The polymer component of the PFNPG composite used in studies described in this chapter, consists of the polymethylmethacrelate (PMMA) modified with low molecular additives and activated with deferent type functional organic compounds [26]. A nature of the latter is chosen depending on a concrete function of the optical element (lasing, Q-switching, etc).
A procedure of making the composite consists of the following stages.
First, a monomer composition is prepared. This stage includes distillation, adding a low molecular modificator, a polymerization initiator, and the functional organic compounds.
Second, a NPG element is inserted into the monomer composition. At this stage NPG pores are quickly filled with the monomer composition due to the capillary effect.
Third, a free-radical polymerization is conducted at 30÷100°C.
The PFNPG samples, obtained in these three stages, are annealed and polished to get an optical element.
In a practical realization of PFNPG procedure, described above, some requirements have to be satisfied. Among these requirements the most important ones are the following.
A preparatory annealing of the NPG samples has to be done to remove molecules adsorbed on the pore surface. The annealing process has to be carried out in well-controlled conditions to avoid collapsing the pore. At the polymerization stage temperature regime has to be also well-controlled to avoid thermally induced stresses leading to peeling the polymer from the pore surfaces. Analyzing the polymerization process in nanoscale pores we have to point out that a structure of the polymer synthesized in the pores can be rather different from that of a bulk polymer synthesized at "open" conditions. In particular, crystallites, globules and other structural elements forming in such "the open" conditions can not be formed at the polymerization in nanopores.

4. Properties of PFNPG

4.1 Samples for investigation

All the data of the investigation results presented below have been obtained on the PFNPG samples made by the technology described briefly in Section 3 above. The NPG, the cage of PFNPG composite, has been made from the glass of the initial content $59.0SiO_2 \times 33.2B_2O_3 \times 4.0Na_2O \times 3.8K_2O$. Porosity of the NPG samples was $P \cong 43\%$, the pore size distribution was single modal with the average pore size $d \cong 7$ nm (see Fig.1). The polymer component of the PFNPG was the modified polymethylmethacrelate (MPMMA). The optical transparency range of the PFNPG samples, limited by the transparency range of the polymer component, was 300÷1600 nm [29] (transparency range of the silica cage component is 200÷2700 nm [30]).
A microscopic testing showed high optical quality of the PFNPG samples: no visual defects were observed.

4.2 Mechanical properties and surface structure of optical elements

Microhardness of the PFNPG (and MPMMA for comparison) was measured using the method described in [31]. The samples were loaded at 1 N during 50 sec. Results of these measurements: the microhardness of the PFNPG composite was 1500÷2000 N/mm², whereas the microhardness of the MPMMA was in factor of 15÷20 less. For comparison: the microhardness of the sodium-borate glass and the quartz glass are 5000 N/mm² and 7000 N/mm² respectively [31]. It has been found that the microhardness of the PFNPG does not depend, in contrast to MPMMA, on contents of the polymer component of the composite, and, hence, is determined by the microhardness of the nanoporous glass.

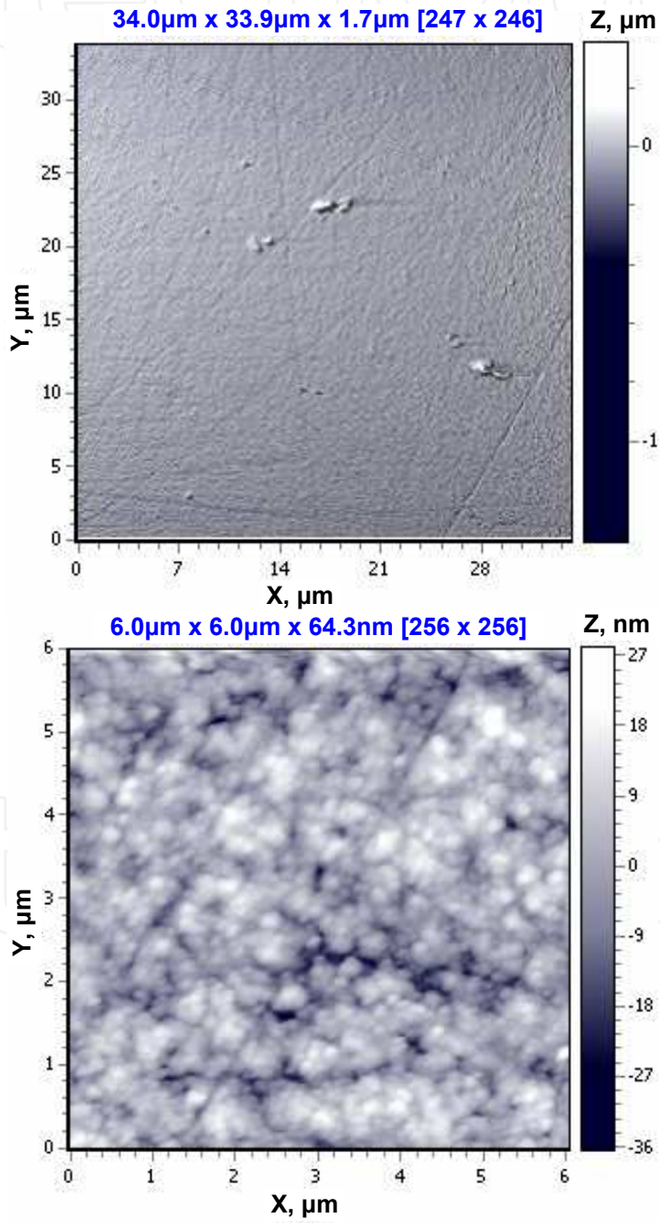

Fig. 2. Surface morphology of the PFNPG sample recorded on AF-microscope with the scan apertures 35×35 µm (top) and 6.5×6.5 µm (bottom). (After Ref. [20].)

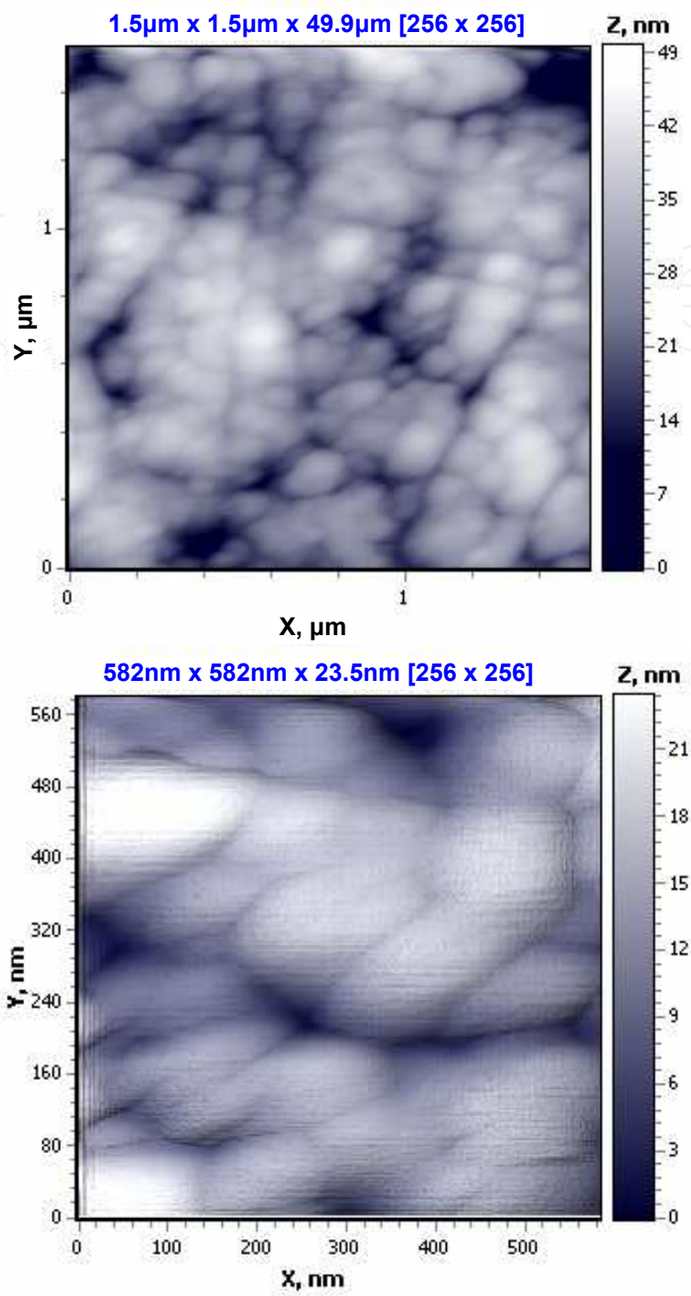

Fig. 3. Surface morphology of the PFNPG sample recorded on AF-microscope with the scan aperture 1.3×1.3 µm (top) and 0.3×0.3 µm (bottom). (After Ref. [20].)

Results of data processing of such the patterns characterized by parameters *Ra* – mean deviation from "ideal" surface, and *Sm* – mean step of roughness, for two PFNPG samples are presented in Table 2.

Three types of the structure defects are seen Fig.2 and Fig.3 on the PFNPG surfaces when the scan aperture varies: at 35×35 µm aperture – chain roughness and scratches on the smooth surface, and at 6.5×6.5 µm aperture – nanostructure of the surface.

Scan aperture, μm	Sample 1		Sample 2	
	Ra , nm	*Sm* , nm	*Ra* , nm	*Sm* , nm
35 × 35	10.5	1642	8.8	1004
6,5 × 6,5	5.9	467	5.7	480
1,3 × 1,3	4.0	345	4.9	411
0,3 × 0,3	1.9	63	2.5	139

Table 2.

A nature of these surface defects and their connection with polishing technology is not clear yet, and further studies are required to clarify this problem.

4.3 Light scattering

The PFNPG composite is a heterogeneous medium. The refractive index difference of the quartz cage and the polymer component may be as high as $\Delta n \cong (2 \div 3) \times 10^{-2}$ (this estimate is based on the assumption that the refractive index of the polymer component in the NPG pores is the same as in the bulk polymer). Such the difference may lead to the significant light scattering losses. For estimation of these losses let us consider the following simple model of the PFNPG composite.

We will consider the two-component composite as "colloidal solution" consisting of spherical polymer inclusions, corresponding to pore sizes, homogeneously distributed in the quartz matrix. A single inclusion light scattering cross-section at $r << \lambda$ (r is pore radius, λ is radiation wavelength) may be obtained from the Raleigh approximation [32]

$$\sigma = \frac{8}{3}\pi k^4 \left| \frac{n_1^2 - n_2^2}{n_1^2 + 2n_2^2} \right| V \tag{1}$$

where k is the wave number, V is the pore volume, n_1 and n_2 are refractive indexes of the quartz matrix and the polymer, respectively. At $n_1 \sim n_2 >> \Delta n$ the relationship (1) is simplified:

$$\sigma = b \times 10^5 \frac{r^6}{\lambda^4} \left(\frac{\Delta n}{n} \right)^2 \tag{2}$$

where n is the refractive index of the quartz, b is a numerical coefficient of the order of 1.

Light scattering-produced losses are characterized by the extinction coefficient $h = N\sigma$, where N is a concentration of scattering particles. For example, at porosity $P = 40\%$, $r = 3.5$ nm, $\Delta n = 3 \times 10^{-2}$, $n = 1.5$ and $\lambda = 500$ nm we get $h \cong 10^{-2} \div 10^{-3}$ cm-1. This rather high extinction doesn't agree with the experimental data for PFNPG samples we studied (much lower losses have been observed). This disagreement indicates that an assumption of independent scattering by each particle is not fulfilled in the case of the real PFNPG composite samples. Indeed, that assumption is correct only for low concentration of particles separated by a distance, l, lager than radiation wavelength, λ, whereas in the PFNPG the concentration of pores is very high: their size, r, and interpores distance, l, are

$\cong 7$ nm (i.e. $<< \lambda \cong$ 500 nm). At the conditions $l << \lambda$ particles (pores) scatter the light coherently (due to interference). The number of these "coherent particle" in λ^3 volume is

$$\frac{4}{3}\pi r^3 N \cong 0.4 \Rightarrow N_{coher} \sim \lambda^3 N \sim 0.1\left(\frac{\lambda}{r}\right)^3 \sim 10^5 \quad (3)$$

Such the high-concentration particle medium can be characterized by an effective refractive index $\bar{n}$ and, according to Ewald-Oseen theorem [33], will produce a low scattering only at small angles in the propagation direction.
Investigation of the small-angle light scattering in the PFNPG composite and the MPMMA bulk polymer samples have been carried out using a setup shown in Fig. 4.

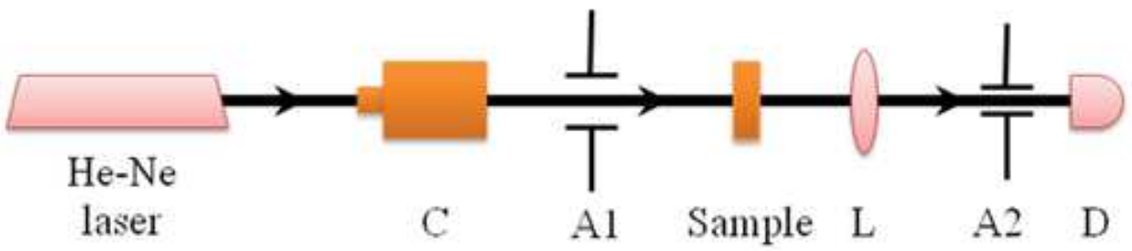

Fig. 4. Schematic of the experiment for investigating small-angle light scattering. **C:** collimator, **A1:** input diaphragm, **L:** collecting lens, **A2:** limiting diaphragm, **D:** photodetector. (After Ref. [12].)

The 633-nm He-Ne laser was used as a radiation source. The laser beam was expanded with a collimator (C) and was limited by an output diaphragm (A1) of the diameter 1 cm. The collimated laser beam was transmitted through a sample, focused on a diaphragm (A2) of a small diameter ϕ, and detected with the photodetector (D). The dependence of the transmitted radiation intensity on ϕ obtained for a number of PFNPG samples and a reference MPMMA sample are shown in Fig. 5.
As is seen in Fig.5 the transmittance of MPMMA does not depend on the diaphragm aperture. This means that scattering losses in this material is negligible (a deviation of the transmittance from unity is due to Fresnel refraction from the sample surfaces). The aperture size dependence of the transmittance observed for PFNPG samples indicates that small-scale inhomogeneity losses are also very low (except for a sample fabricated by "non-perfect" technology) , but large –size inhomogeneities responsible for a transmittance decrease at ϕ <150 μm rather significantly reduce the transparence of the samples. A size, $\bar{D}$, of these inhomogeneities can be estimated from the elementary diffraction theory:

$$\bar{D} \sim f\frac{\lambda}{d} \sim 4\times 10^{-3} f \quad (4)$$

where f is a focal length of the lens, d is the diaphragm aperture size at which the transmittance decrease is observed. Taking concrete parameters of the setup and experimental data, the values of $\bar{D}$ in PFNPG samples studied have been estimated as $\bar{D} = 1 \div 3$ mm.

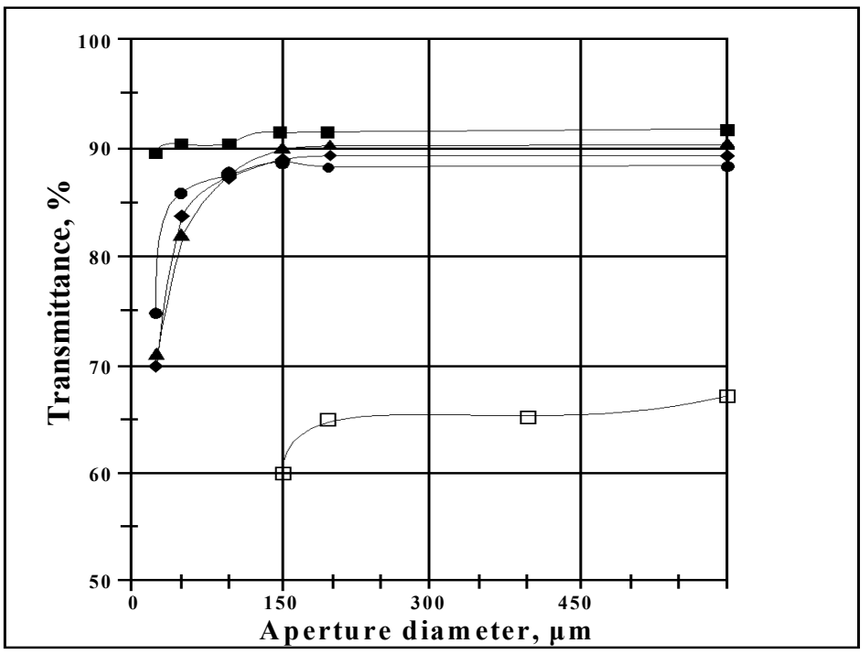

Fig. 5. Transmittance of the samples versus limiting diaphragm aperture
■ is MPMMA doped with PM-597 dye; ◆ is PFNPG doped with PM-580 dye; ● is PFNPG doped with PM-597 dye; ▲ is PFNPG doped with 11B dye; □ is PFNPG sample fabricated by with "non-perfect" technology. (After Ref. [12].)

An analysis of these data has shown that scattering in the PFNPG samples studied is due to large-scale inhomogeneities associated with the sample making technology. This is especially seen for the PFNPG sample fabricated by "non-perfect" technology.
Detail studies of optical inhomogeneity of PFNPG samples were performed using interferometric holography [34]. Schematic of experimental setup is shown in Fig. 6

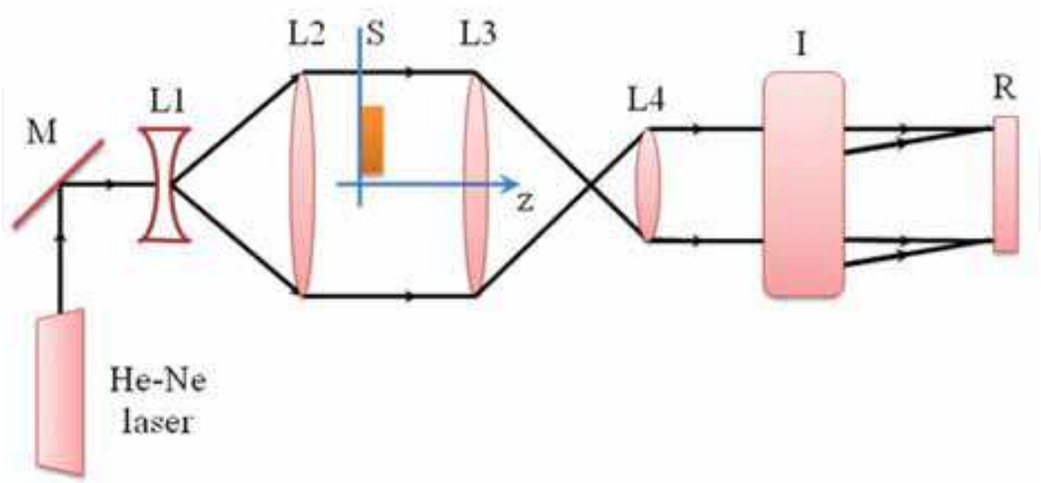

Fig. 6. Schematic of experimental setup for holography recording: **He-Ne** laser, **M:** mirror; **L1** and **L2:** telescopic system for beam forming, **S:** sample under study, **L3** and **L4:** input beam system, **I:** interferometer, **R:** hologram recording plate

Schematic of a hologram restoration is shown in Fig. 7.

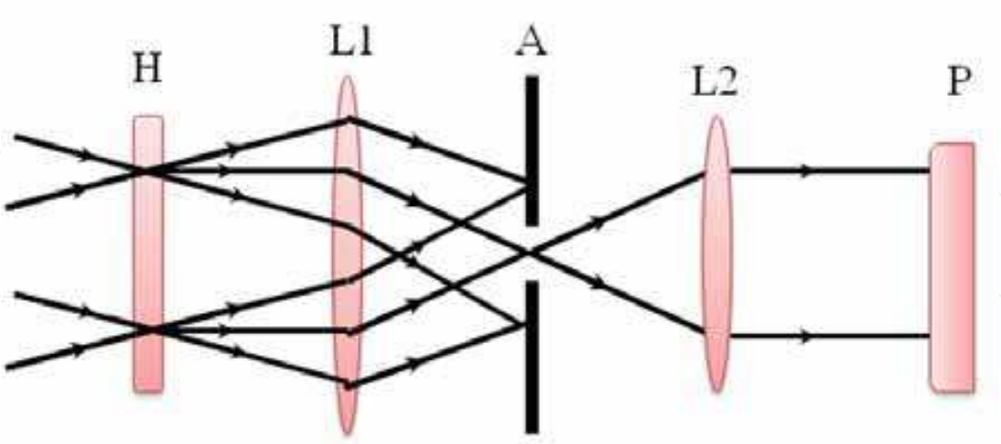

Fig. 7. Schematic of hologram restoration: **H:** hologram, **L1** and **L2:** focusing lenses, **A:** aperture, **P:** registration plate

Typical interference patterns of PFMPG sample are shown in Fig. 8.

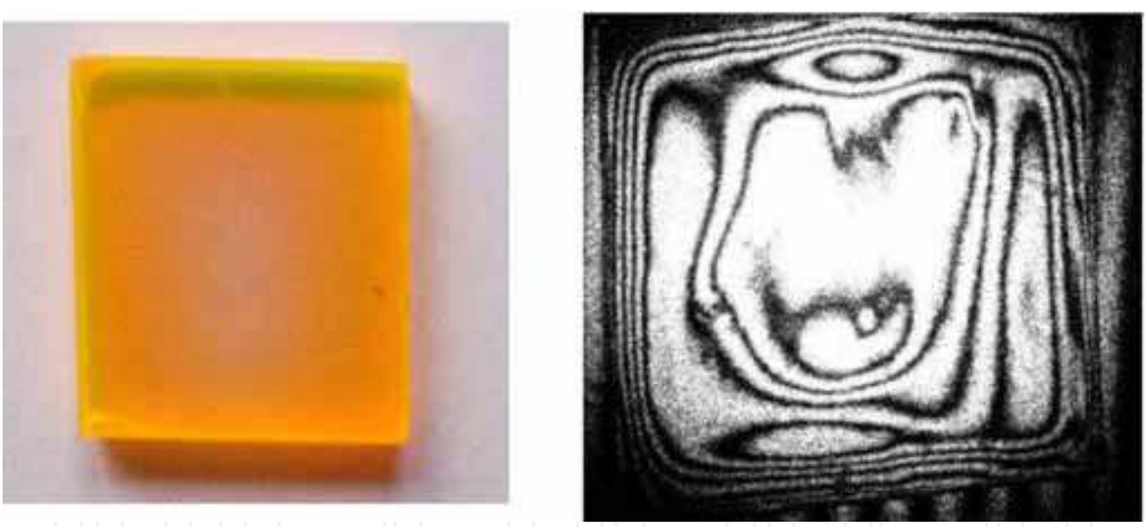

Fig. 8. PFNPG sample (left) and its interference pattern (right). (After Ref. [20].)

Result of these interferometic studies has shown that PFNG samples have high optical quality: the optical length difference in a central part of the sample doesn't exceed $0,02\lambda$ that corresponds to the refractive index variation $\delta n \le 10^{-6}$. A rather large variation of the refractive index observed only in the periphery of the sample is due to structural changes associated with diffusion processes in silica.

4.4 Laser-induced damage resistance of PFNPG

Laser-induced damage of optical materials is important phenomenon limiting the intensity of the laser radiation propagating in optical components of high-power laser systems. Elucidation of the fundamental mechanisms of laser-induced damage in optical materials of

different classes was a subject of many studies during more than 40 years since its first observation [35]. These studies resulted in establishing major features of the phenomenon (dependence of damage thresholds on radiation frequency, pulsewidth, and temperature, statistical behaviour at single-shot and multi-shot irradiation regimes, etc), a development of theoretical models of damage mechanisms and their experimental verification. This allowed working out the effective methods of a significant increase of the damage resistance of many type optical materials including glasses, crystals, and polymers (for a review of these achievements see [36-38] and reference therein).

In particular, it has been reliably established that in a majority of optical materials the laser-induced damage is initiated by absorbing inclusions (it's so called *extrinsic* mechanism), whereas *intrinsic* damage mechanisms (associated with the impact and multi-photon ionization) are realized only in very pure (inclusion-free) materials.

Many experimental facts confirm a dominating role of absorbing inclusions in laser-induced damage (LID) of optical materials. The most pronounced facts are:

- a variation of the damage threshold in samples of the same material obtained by identical technology,
- an increase of the damage threshold with purification of the materials,
- a variation of the damage threshold in different parts of the sample,
- a dependence of the damage threshold on the irradiation spot size.

The theory of the extrinsic laser-induced damage has been well developed and confirmed experimentally [36-40]. In particular, an accumulation effect, reduction of the laser-induced damage threshold at the multi-shot irradiation regime, the most pronounced in polymer material [26], is rather well understood [41-43].

The laser-induced damage in PFNPG has been investigated in both the single-shot and the multi-shot regimes at two laser wavelengths, 1063 nm and 532 nm (Nd:YAG laser and its second harmonic) and pulsewidth 15 ns and 26 ns, respectively. A spatial variation of the damage threshold has been observed indicating an extrinsic nature of damage. The average values of the damage threshold were 70 J/cm^2 and 35 J/cm^2 at 1036 nm and 532 nm respectively [9,12,17,19,24,25]. An influence of technological factors, the purification of the monomer and the impregnation of low molecular additives, on the damage resistance of the PFNPG and MPMMA samples have been also investigated. Results of these studies are shown in Table 3 [9,12,19].

Samples	Monomer purification	Low molecular additive	Single-shot (1×1) threshold, J/cm^2	Multi-shot (1×200) threshold, J/cm^2
MPMMA	-	-	17	1.6-1.9
MPMMA	+	-	63	2.2-2.6
MPMMA	-	+	15	5.4-6.3
PFNPG	-	-	58	31-38
PFNPG	+	-	76	35-43
PFNPG	-	+	56	25-28

Table 3.

The data presented in this table indicate the important features of the laser-induced damage. The damage thresholds of PFNPG in both the single-shot and the multi-shot regimes are

higher of those for MPMMA. The most significant difference is observed at the multi-shot irradiation regime that has a principle advantage for practical applications. It's important also that both the purification of the monomer and the impregnation of the low molecular additives don't affect significantly the damage threshold of PFNPG, in contrast to the bulk PMMA.

These results may be simply explained by the assumption that the laser-induced damage in both materials (PFNPG and bulk MPMMA) has the extrinsic nature, i.e. associated with a presence of absorbing inclusions (this assumption is confirmed, as it had been pointed out above, by the fact of a spatial variation of the damage thresholds). Small-size pores (~ 7nm) in the NPG act as an effective filter for the monomer impregnated to the PFNPG at fabrication procedures. This self-filtration effect reduces the influence of any absorbing inclusions and increases the laser-induced damage resistance.

4.5 Activation of PFNPG with functional organic compounds

Impregnation of functional organic compounds (FOC) into PFNPG to get desirable laser optics elements (lasing, Q-switching, mode-locking, etc) requires special technological studies. The most important requirements to the FOC impregnation technology are as follows. Impregnation procedures have to be consistent with the PFNPG technology. FOC has to be homogeneously distributed in the composite, and does not interact with the composite matrix (NPG cage) to avoid undesirable changes of the properties.

In accordance with the PFNPG technology FOC is dissolved in a monomer composition. However, since NPG cage is an effective adsorbent, due to a very developed pore surface structure, the FOC can strongly interacts with the pore surface and changes the properties. An efficiency of this possible adsorption processes can be, naturally, very different for different types of FOC. Some results of the studies of this problem are presented below. These studies have been carried out with FOC of Pyromethene (PM 567, PM 580, PM 597, PM 650), Phenolemine (Ph 510, Ph 512, Ph 640), and some other series [9,10,13,15,16]. To investigate the homogeneity of FOC distribution in the PFNPG volume, transmittance of He-Ne laser radiation at 633 nm has been studied [12]. The 2 mm diameter laser beam was scanned over a sample surface. Experimental data for the PFNPG sample activated with PM 580 are presented in Fig 9. Similar results have been obtained for other FOCs: PM 597, PM 567, PM 650, Ph 512.

As is seen in Fig.9 the FOC is distributed in the sample rather homogeneously. Location of the FOC in the PFNPG was found to be strongly dependent of its chemical nature: experimental studies of the FOC impregnation process showed that Rodamine 11B strongly adsorbed on pore surface, whereas the FOC of Pyrromethene series do not show the adsorption effect [15].

The efficiency of FOC impregnation to the composite may be characterized by the saturation coefficient $\xi = c_v / c_m$, where c_m and c_v are the FOC concentration in the initial monomer composition and in the PFNPG composite, respectively. A concentration dependence of this coefficient has been investigated by measuring an absorption spectrum intensity of FOC in the monomer solution. It has been found that for all FOC investigated Buger law $D(\lambda) = \ln(I_0 / I) = \varepsilon(\lambda) cL$ is satisfied in a solubility range (here $D(\lambda)$- optical density, $\varepsilon(\lambda)$ and c – extinction and concentration of FOC, respectively, L is sample thickness, I_0 and I are intensities of incident and transmitted radiation, respectively). This means that in the whole solubility range of FOC associates in monomer are not formed. It's important that the

absorption spectra of FOC in the PFNPG composite and in the monomer composition were identical. This indicates that the Buger low is satisfied also for FOC impregnated to the composite, and, hence the saturation coefficient can be determined from the relationship $S = D_c L_m / D_m L_c$ where D_c and D_m are optical densities of the composite sample and FOC solution cell, respectively.

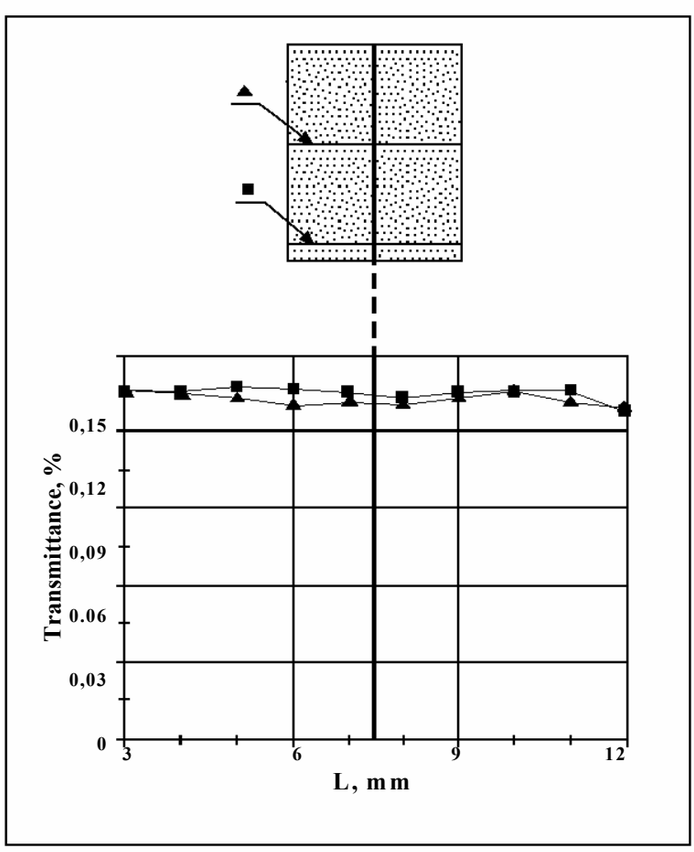

Fig. 9. Transmittance at 543 nm of PM 580 dye-activated PFNPG composite at various sites of the sample. Concentration of the dye in the monomer composition is 2.4 mmol/l. (After Ref. [12].)

Detailed investigations of the saturation process have been carried out for two classes of FOC: Pyromethenes (PM 567, PM 580, PM 597 and 560) ant Phenolemines (Ph 10, Ph 512 and Ph 640). It has been found that for all Pyrromemthene series FOC studied the values of ε are almost the same: $\xi = 0.6 \div 0.7$, and do not depend on a stand time of NPG in the monomer composition. In the contrast, for FOC of Phenolemine series the values of ξ exceed unity (ξ = 1÷1.2 for Ph 512, 1.7÷3 for Ph 510, and 7÷15 for Ph 640) and increase with the stand time of NPG in the monomer composition. Such the behaviour of the saturation coefficient is due to, perhaps, the difference of the dye polarity. In particular, Ph 640 has the ionic form and, taking into account physical-chemical properties of NPG pores [28], it is well adsorbed on the pores surfaces. Therefore, one may conclude that low polarity FOC (PM 567, PM 580, PM 597, PM 650) do not incline to adsorption on the pore surface, that correlates with rather

low saturation coefficients, whereas the high polarity FOC, especially having the ionic form, are well adsorbed on the pore surface.

4.6 Optical distortions

A dependence of the refractive index of optical materials on different external factors is the important characteristic for many laser applications. Two dependences, on temperature and intensity, are most significant in high-power laser optics. They can induce significant undesirable distortions: divergence, self-focusing or self-defocusing of optical beams.

Thermo-optical effects associated with the temperature dependence of the refractive index (dn/dT) can be characterized by the thermo-optical figure of merit $\mu = \chi(dn/dT)^{-1}$. A thermo-optical lensing induced by the inhomogeneous laser-produced heating is determined by this parameter: a higher value of μ corresponds to lower optical distortions.

Thermo-optical distortions in the PFNPG composite have been investigated by measuring the focal length of the thermal lens induced by a propagating laser beam [12]. For comparison similar measurements have been done also for the bulk MPMMA samples. Schematic of the experiment is shown in Fig 10.

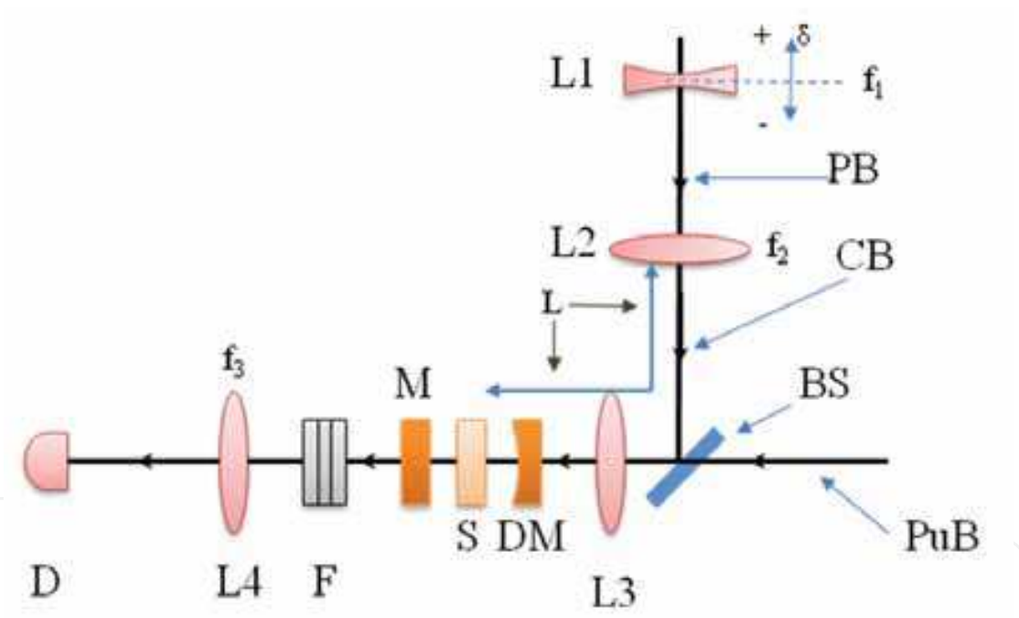

Fig. 10. Schematic of experimental setup for laser-induced thermal lens studies: **D:** photodetector, **L4:** lens, f_3=1000 mm, **F:** light filter, **M:** output cavity mirror, **S:** sample under study, **DM:** dichronic mirror, **L3:** large-aperture lens, **PuB:** pump beam (λ=532 nm), **BS:** beam splitter, **CB:** collimated beam, **L2:** lens f_2=300 mm, **PB:** He-Ne laser probe beam, **L1:** lens f_1=-25 mm. (After Ref. [12].)

The probe beam from a He-Ne laser (PB) at 633 nm was expanded with a collimator consisting of a diverging lens with the focal length $f_1 = -25$ mm (L1) and a converging lens with the focal length $f_2 = 300$ mm (L2). The beam cross section was limited by the 5 mm diaphragm. The pump beam (PuB) at 532 nm passed through the same diaphragm. Both beams were incident on a laser element (S) under study. The pump beam transmitted

through the laser element was rejected with a filter (F), and the probe beam was focused with a lens (L4) of the focal length $f_3 = 1000$ mm on a photo-detector (D). The lens (L1) with the focal length f_1 was displaced to obtain the maximum signal from the detector in the absence of the pump.

Upon pumping the output signal decreased due to defocusing of radiation by a thermally induced lens. Displacing the lens L1 by some distance δ one can get the signal increased to maximum. The value f_T is related to δ by the simple expression from geometrical optics:

$$f_T = (L - f_2) - f_2^2 / \delta \tag{5}$$

where L is a distance from the L2 lens to the laser element.

Thermo-optical effects were studied in the laser elements doped with the PM 597 dyes, which absorbed the radiation at 532 nm. The dependence of f_1 on the average absorbed pump power was measured for the PFNPG laser element and the reference MPMMA element. The study showed that thermo-optical effects in the PFNPG composite are much weaker than those in the MPMMA (see Fig. 11).

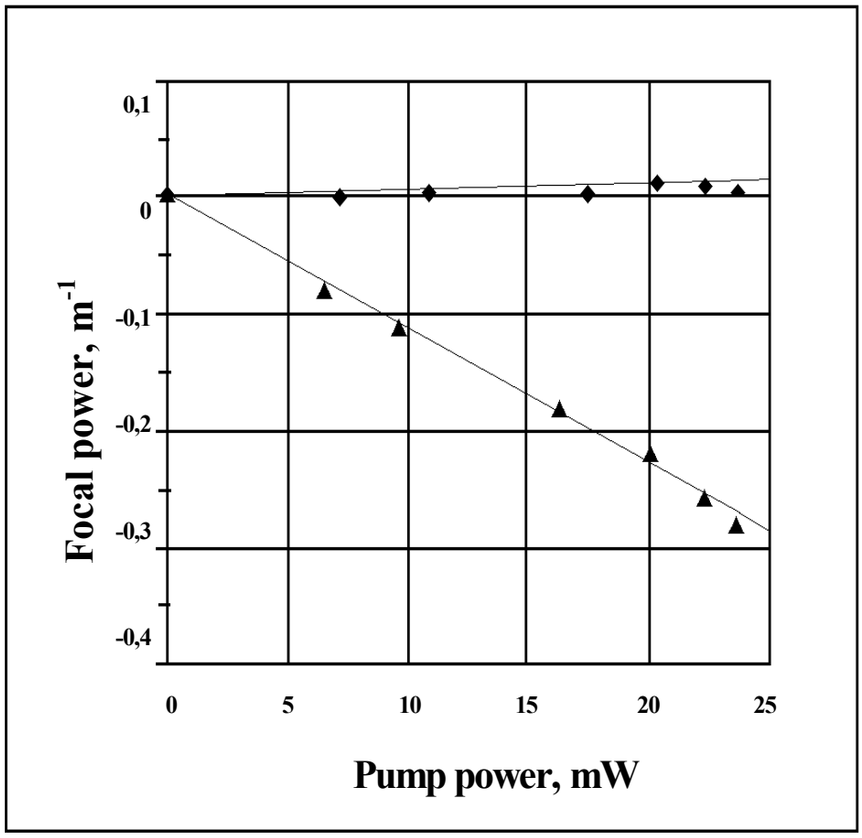

Fig. 11. Focal power dependence of the thermo-optical lens versus the average pump power for the PFNPG element (◆) and the reference MPMMA element. (▲). (After Ref. [12].)

The advantages of the composite over the bulk PMMA are caused by a number of factors. The main one is a considerably lower magnitude of dn/dT. Indeed, according to the Lorentz – Lorentz relation [33], the molar refraction index, R, is

$$R = \frac{M}{\rho}\frac{n^2-1}{n^2+2} \tag{6}$$

where M is the molar mass and ρ is the material density.
By differentiating (6) with respect to temperature and taking into account that M and R are independent of the temperature we obtain [12]:

$$\frac{dn}{dT} = -\alpha\frac{(n^2-1)(n^2+2)}{2n} \tag{7}$$

where α is the linear expansion coefficient of the material.
For PMMA $\alpha \cong 7\times10^{-5}$ K^{-1} [29]. Being impregnated into glass pores, PMMA cannot expand freely because of quartz cage limitations. This means that PMMA in the NPG pores expands with the temperature increasing in the same way as cage pores do. In this case, to estimate the value of dn/dT of PMMA impregnated into the NPG, one should use in (7) the linear expansion coefficient of fused silica, i.e. take the value $\alpha \cong 0.51\times10^{-6}$ K^{-1} [44]. Therefore the value of the dn/dT for the PFNPG composite is by factor of 100÷130 times lower than that for the bulk PMMA.
The second important factor, which reduces thermo-optical effects in the PFNPG composite as compared to PMMA, is the high thermal conductivity of the quartz cage of the composite. The thermal conductivity coefficient for quartz and PMMA are 1.3 and 0.16 kcal h^{-1} m^{-1} K^{-1}, respectively [30], so that their ration is approximately equals to eight. Taking into account that the glass porosity is 40% this ratio means that thermo-optical effects should be reduced by a factor of 4÷5.
Thus, the thermo-optical figure of merit of the PFNPG is a factor of 500÷600 times larger than that for the bulk PMMA.
A nonlinear refraction of PFNPG samples has been also investigated. A traditional Z-scan techniques [45] was used in the experiments. A setup and experimental details will be presented in the Section 5 below. Here we summarize only the results of these studies in comparison with data obtained for MPMMA. It has been found that PFNPG doesn't reveal an appreciable nonlinear refraction in the contrast to the bulk MPMMA that has a significant nonlinear susceptibility. Further studies are required to understand a reason for these results.

5. Laser applications of PFNPG elements

The PFNPG composite as a host material allows making laser optics elements of different types by varying a content of functional organic compounds impregnated. The Q-switchers [1, 8-10], lasing elements [11, 13-21], and laser radiation power limiters [22-25] have been made and successfully demonstrated to date. Other elements, such as the mode-lockers, can be also made by choosing a proper FOC. Below in this section some experimental results on lasing and power limiting properties of PFNPG are presented.

5.1 Absorption and luminescence spectra features of dye-impregnated PFNPG

PFNPG samples activated with Pyrromethene (PM-567, PM-597 and PM-560) and Phonolemine (Ph-510, Ph-512 and Ph-640) series dyes have been investigated. These dyes were chosen since they possess a high lasing efficiency in liquid solutions and widely used in experimental practice.

Dependence of absorption spectra of all these dyes has been investigated at different concentrations in the monomer and in the PFNPG composite. The concentration was varied in the wide range, from 10^{-5} mol/l to a solubility limit. Data on the solubility limit, C_s, characteristic luminescence quenching concentration, C_a, and "spectral shoulder" of a luminescence lines, C_{ex}, of some dyes in the monomer solutions are presented in Table 4.

Dye	PM567	PM580	PM597	PM650	Ph512	Ph510
C_s, mol/l	2×10^{-2}	2.2×10^{-2}	2×10^{-2}	1×10^{-2}	1×10^{-2}	0.5×10^{-2}
C_e, mol/l	1×10^{-2}	1×10^{-2}	1×10^{-2}	0.5×10^{-2}	2.5×10^{-3}	1×10^{-3}
C_{ex}, mol/l	1×10^{-3}	1×10^{-3}	1×10^{-3}	1×10^{-5}	1×10^{-3}	1×10^{-3}

Table 4.

Main results of the studies may be formulated as follows.

1. Absorption spectra of all dyes investigated in the monomer solutions remain unchanged in a whole concentration range, up to the solubility limit and Buger law is fulfilled. It means that dye associates are not formed. Typical absorption spectrum for PM-650 is shown in Fig. 12.

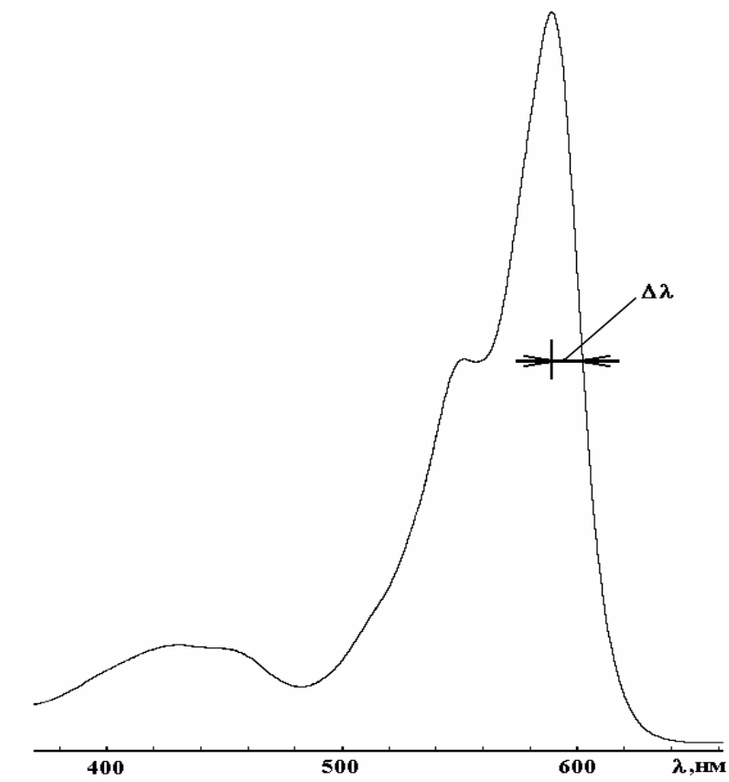

Fig. 12. Absorption spectrum of PM-650 in the monomer composition

Some spectral characteristics of dyes important for understanding their lasing properties are presented in Table 5.

Dye	λ_a, nm	λ_f, nm	$\Delta\lambda$, nm	$\varepsilon(\lambda_a)\times10^{-3}$	$\varepsilon(\lambda_p)\times10^{-3}$	$\varepsilon(\lambda_f)\times10^{-3}$
PM 567	518	536	10	96	28	14
PM 580	520	537	10	89	32	16
PM 597	524	561	16	80	64	3
PM 650	590	607	14	45	14	14
Ph510	524	593	46	22	21	1.5
PH512	533	578	24	25	25	2
Ph640	590	616	16	30	8.5	5.5

λ_a, λ_f, и λ_p are wavelengths of main pick of absorption and luminescence lines and pump respectively, $\varepsilon(\lambda)$ is an extinction, $\Delta\lambda=(\lambda_{1/2}-\lambda_a)$, $\lambda_{1/2}>\lambda_a$,, $\varepsilon(\lambda_{1/2})=(1/2)\ \varepsilon(\lambda_a)$.

Table 5.

2. Absorption spectra of the dyes impregnated to PFNPG composite are identical with those in the monomers mixture. This result is natural for Pyromethene dyes since the saturation coefficient (characterizing impregnation efficiency) $\xi<1$, so that the dyes located (as it has been discussed above in Sec. 4) in a volume of the polymer component. However, the identity of absorption spectra in PFNPG and in monomer mixture for dyes possessing high ($\xi>1$) saturation coefficients is not clear since this fact ($\xi>1$) indicates a strong interaction of dye molecules with the pore surface and has to lead to absorption spectrum change.
3. In the contrast to the absorption spectra features, just discussed above, luminescence spectra of dyes both in monomer solutions and impregnated to PFNPG, reveal a concentration dependence: at high concentrations, exceeding C_{ex}, a "spectral shoulder" appears at the long-wavelength side of the luminescence line. Such a behaviour of the luminescence spectra evidences, perhaps, of an eximer formation at high concentrations of the dyes.
4. At high dye concentrations (> 10^{-3} mol/l) in the monomer solution a luminescence quenching is observed (see, Fig 13).

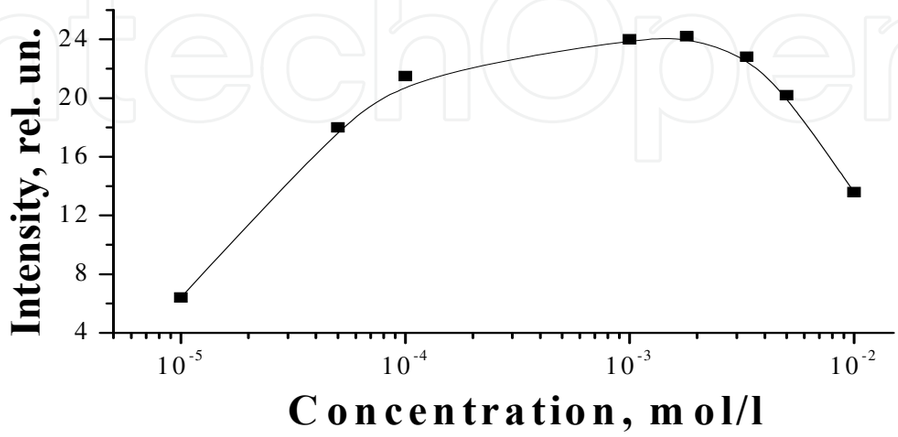

Fig. 13. Luminescence intensity versus dye concentration of Ph-512 in the monomer solution

5. An increase of the luminescence intensity is observed for the dyes impregnated to PFNPG as compared with the monomer solutions. This effect is due, perhaps, to a suppression of non-radioactive relaxation.

5.2 Lasing properties

Lasing characteristics of the dye-impregnated PFNPG composite have been investigated using experimental setup shown in Fig. 14.

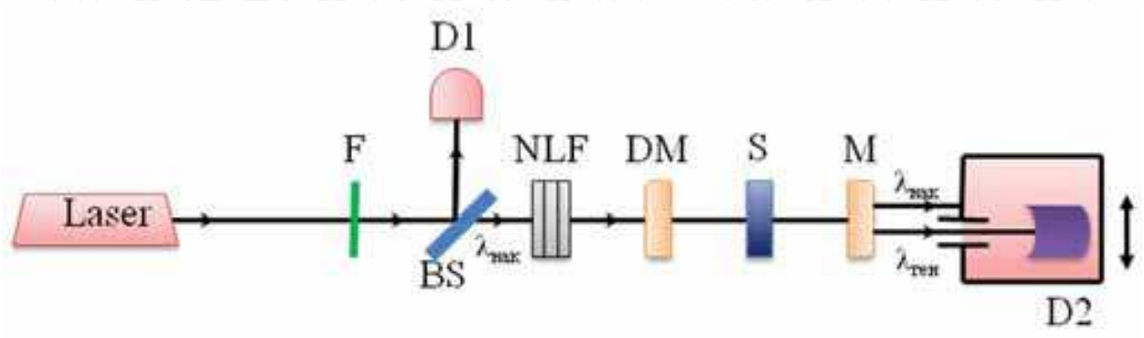

Fig. 14. Schematic of setup for investigation of lasing characteristics of dye-impregnated PFNPG elements. **F**: light filters **BS**: beam splitter, **NLF**: neutral light filters, **DM**: dichroic mirror, **S**: sample, **M**: mirror, **D1**: photodiode detector and **D2**: photodiode detectors or wavelength-meter

The pump source was a frequency-doubled Q-switched Nd: YAG laser. The longitudinal pumping scheme was used. A laser element (S) was placed into a cavity formed by a dichroic mirror (DM), transparent at the pump wavelength, λ_p =532 nm, and totally reflecting at the lasing wavelength, λ_g. The pump beam diameter at the laser element was 1.3 mm. The repetition rate, f, of the pump pulses was 3 Hz or 33 Hz., and the duration, τ_p, energy, E_p, and intensity, I_p, were 5 ns, 2mJ, and 30mW/cm² at $f = 3$ Hz, and 7ns, 0.7 mJ, and 7.5 MW/cm² at $f = 33$ Hz, respectively.

The pump–to–laser conversion efficiency, η, and the service life, $N_{0,7}$, defined as a number of pulses at which η drops to the 0.7 level of its maximum value at the first pump pulse, were measured in a broad range of the pump intensity variation. Also, the dependences of η and $N_{0,7}$ on the pump pulse reprate were investigated.

The conversion efficiency was determined as the ratio $\eta = \left(E_g / E_P\right)$ of the lasing pulse energy, E_g, to the pump pulse energy, E_P. The investigation of the dependence of the conversion efficiency on the optical density, D, of the laser elements has reviled its non-monotonous character. The typical shape of $\eta(D)$ observed for the PM597 dye-doped PFNPG element is shown in Fig.15. An existence of the optimal optical density, D_m, corresponding to the maximum value of the conversion efficiency, is explained as associated with the inhomogeneous pumping of the laser element. Indeed, at the longitudinal pumping condition, which took place in the experiments described above, the pump intensity gradually decreases from a front surface of the laser element to a back one if the optical

density of the element is high enough. Therefore, at high densities, $D > D_m$, a region adjacent to the back surface remains "unpumped" and reabsorption processes at a laser transition reduce the lasing efficiency.

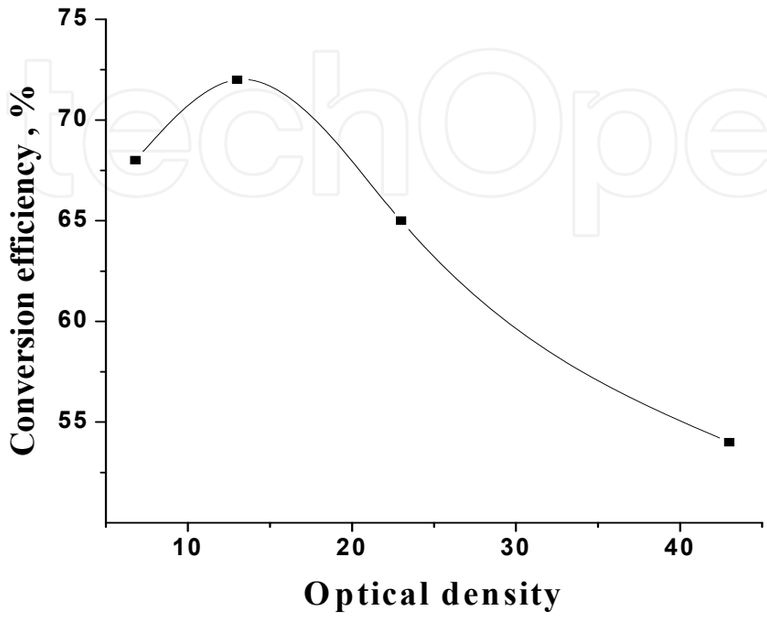

Fig. 15. Lasing conversion efficiency versus optical density of PM597 dye-doped PFNPG element pumped at λ_p =532 nm, I_p =30 MW/cm^2. (After Ref. [16].)

Experimental data for the conversion efficiency and the service life obtained for PFNPG elements doped with some Pyrromethene and Phenolemine families dyes are presented in Table 6.

Dyes	PM567	PM580	PM597	PM650	PH512	Ph510	Ph640
λ_g , nm	562	561	570	625	595	614	642
D_m	8.8	12	13	1.6	5.8	10	4.3
η_m (%)	55	55	72	33	42	30	35
$N_{0,7}\times10^3$	40	51	340	8	30	14	16

Table 6.

This data refer to elements with optimal optical densities ($D = D_m$) and have been obtained at the pump pulse reprate 33 Hz.

It has been observed that at the lower reprate, 3 Hz, the conversion efficiency for PFNPG elements remained unchanged and the service life increased in a factor of 2-3. The different behaviour has been observed for dyes dissolved in liquid solutions (monomer mixtures and ethanol): the conversion efficiency measured at the same pumping conditions, decreased at the higher (33 Hz) reprate. This result definitely demonstrates the advantage of the solid-state PFNPG laser elements over the liquid solution dye lasers.

5.3 Nonlinear absorption

Nonlinear absorption in the functional organic compounds was investigated since 80-th of the last century. These studies were motivated by needs to create the laser radiation power limiters for protection of receives (including eyes).

A majority of studies were carried out on liquid solutions of the FOC. However, for practical applications solid-state limiters are, naturally, more preferable. In this respect the PFNPG is a very suitable candidate for such power limiters. Taking into account this, the nonlinear absorption properties of some organic compounds impregnated to PFNPG have been recently studied [22-25].

Compounds of Phthalocyanine and Porphyrin families containing "heavy" atoms have been chosen for these studies since they showed the most suitable nonlinear properties in liquid solutions [46-49]. In particular, Zinc Porphyrin (PrZn), Zinc Phthalocyanine (PcZn) and Lead Phthalocyanine (PcPb) dyes have been chosen. The solubility limits of these compounds in the monomer solution are 5 mmol/l for PrZn and 1 mmol/l for PcZn and PrZn.

The absorption spectra of these compounds in monomer solutions and in PFNPG have been found identical in the whole concentration range up to solubility limits.

The samples of the bulk MPMMA impregnated with these dyes have been also studied for comparison.

Optical densities at 532 nm of the samples studied are presented in Table 7.

Sample	PFNPG PrZn	PFNPG PcZn	PFNPG PcPb	MPMMA PcZn	MPMMA PcPb
Optical density at 532 nm	0.58	0.24	0.38	0.5	0.8

Table 7.

Before presenting experimental data let us discuss briefly a possible mechanism of nonlinear absorption in the chosen compounds.

It is supposed that the nonlinear absorption in these compounds is due to radiation-induced triplet-triplet absorption [46-49]. An energy level diagram shown in Fig. 16 explains this mechanism.

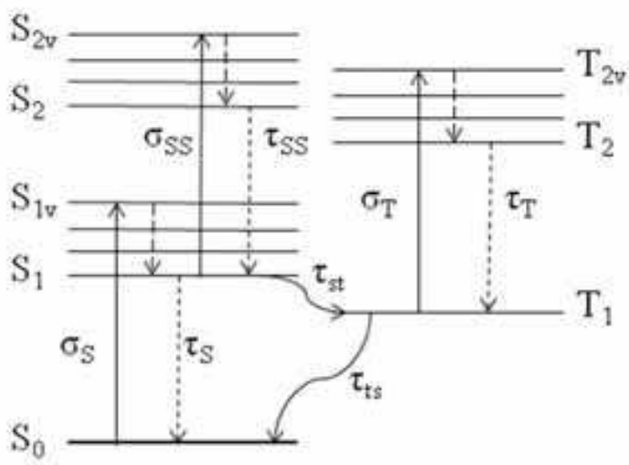

Fig. 16. Energy level diagram of organic dyes

A high power laser radiation at a resonant frequency corresponding to $S_0 \to S_{1v}$ transition, increases a population of the triplet state T_1 and induces the electromagnetic transitions between two triplet states $T_1 \to T_{2v}$. If the cross-section, σ_T, of the $T_1 \to T_{2v}$ transition exceeds the cross-section, σ_S, of the $S_0 \to S_{1v}$ transition, a transmittance of the sample at the laser frequency (transition $S_0 \to S_{1v}$) will be decreased, i.e. will lead to laser radiation power limiting. Besides this darkening mechanism, due to the triplet-triplet absorption, other mechanisms are possible (for example, due to $S_1 \to S_{2v}$ transition). However, in the organic dyes containing heavy atoms, the mechanism, just described above, is supposed to be dominant one.

Experimental studies of nonlinear absorption were carried out using Z-scan technique [24,25]. Schematic of the setup is shown in Fig. 17.

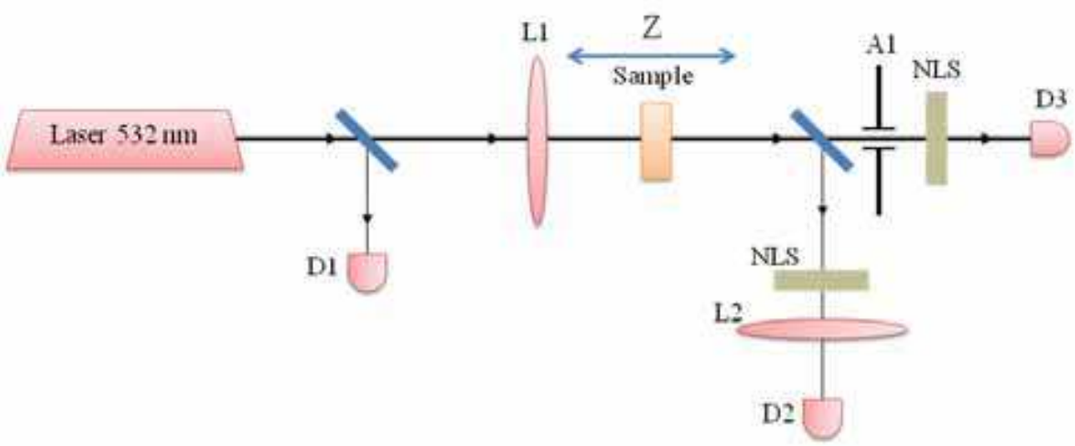

Fig. 17. Schematic of setup for investigation of nonlinear absorption: **A1:** diaphragm ∅3,5 mm, **L1:** lens (focal length 135 mm), **D1, D2** and **D3:** photodiode detectors, **NLF:** neutral light filters. (After Ref. [25].)

The second harmonic of the single mode, 40 ns – pulse duration Nd:YAG – laser has been used as a light radiation source. The radiation beam focused by 135 mm focal length lens, L1, passed through a sample under study, registered by the detector D2.

The nonlinear absorption in the sample was registered in "wide aperture configuration" (when whole beam was detected) when it scanned along the propagation direction. The nonlinear refraction was registered in the "narrow aperture configuration" (when 3.5. mm aperture diaphragm limit the transmitted beam diameter) by the detector D3.

The nonlinear absorption has been revealed in all samples studied. Typical transmission curves observed at the "wide" and "narrow" configurations in the PcPb sample are shown in Fig. 18.

As is seen, both the left and the right curves are symmetric relative to the focal position of the sample. This definitely indicates an absence of the nonlinear refraction in The PFNPG samples.

Different Z-scan plots have been detected in the bulk PMMA samples doped with the same dye: the symmetric shape plot in the "wide aperture" configuration and the asymmetric one – in the "narrow aperture" configuration (Fig. 19). This result indicates a presence of the nonlinear refraction in the PcZn-doped PMMA polymer.

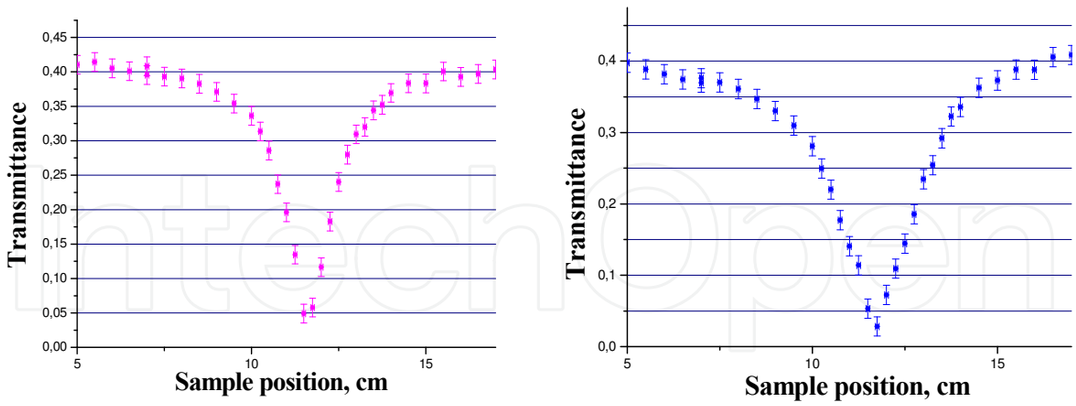

Fig. 18. Transmission versus Z-position of the sample made of PFNPG doped with PcPb, observed in wide aperture (left) and narrow aperture (right) configuration (After Ref. [25].)

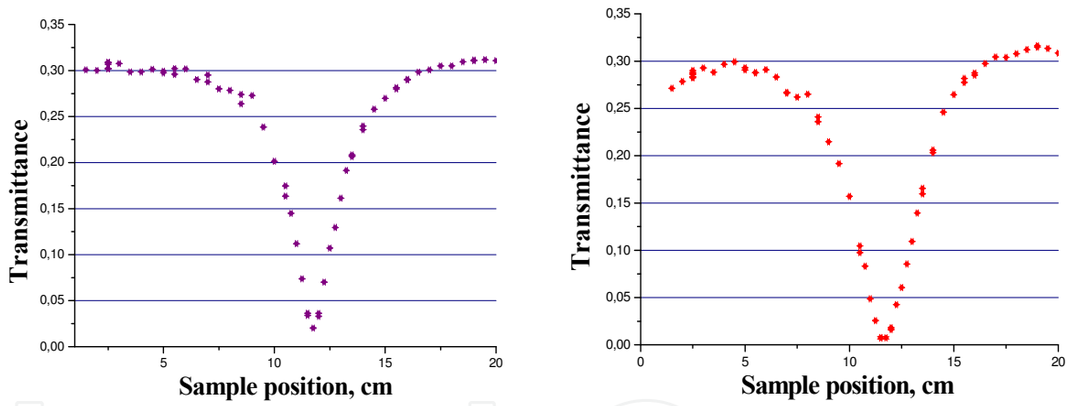

Fig. 19. Transmission versus Z-position of PcZn-doped PMMA sample, observed in "wide aperture" (left) and "narrow aperture" configurations. (After Ref. [25].)

To understand the difference of the nonlinear refraction properties of the PFNPG and the bulk PMMA polymer, the dye-free samples made from these materials, have been studied in "narrow aperture" Z-scan configuration. Z-scan curves observed in this case are shown in Fig. 20.

The important feature of these results is that the nonlinear refraction is definitely detected in the bulk PMMA polymer, where as it does not revealed in PFNPG composite at the same experimental conditions.

Note the other interesting results obtained in Z-scan experimental studies of dye-doped PFNPG: no laser-induced damage has been revealed at the laser radiation energy densities up to 4 J/cm², but destruction of the dyes has been observed at lower energy densities, beginning at 2 J/cm².

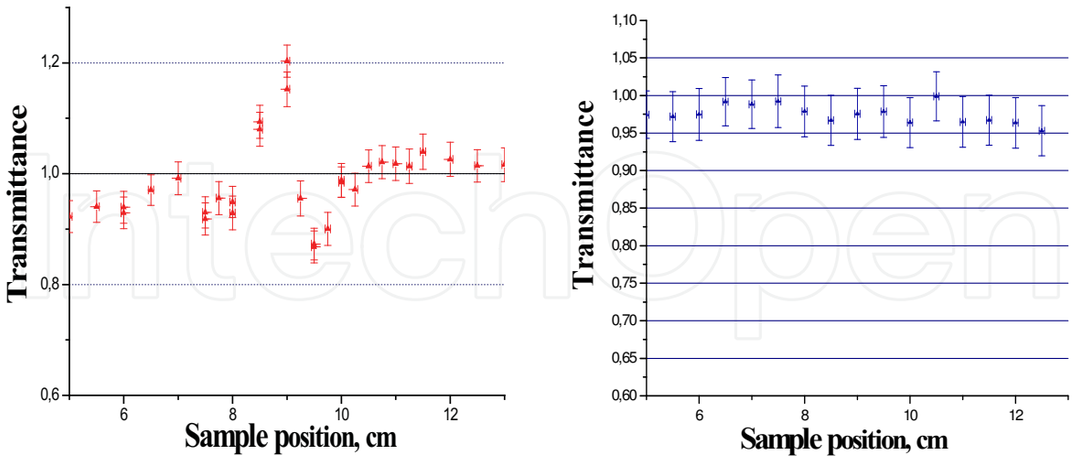

Fig. 20. Transmission versus Z-position of dye-free bulk PMMA polymer (left plot) and PFNPG composite (right plot) samples. "Narrow aperture" configuration. (After Ref. [25])

Characteristics of the nonlinear absorption in the dye-doped PFNPG have been studied using other experimental setup shown in Fig.21. The transmittance of the samples was measured at a wide range of the laser radiation intensity [22,23].

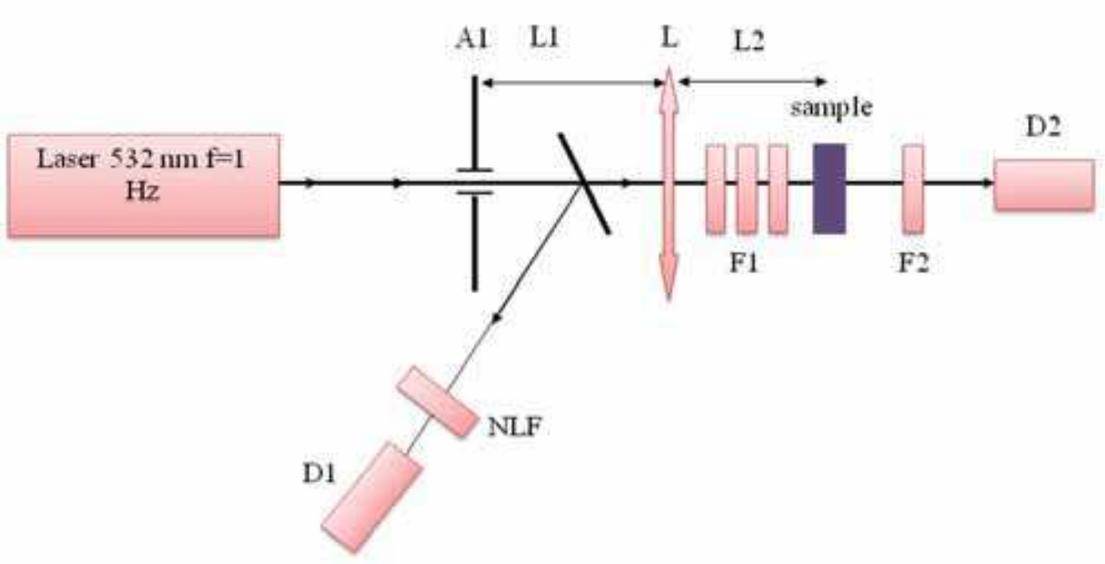

Fig. 21. Schematic of setup for investigating nonlinear absorption: **D1** and **D2:** photodetectors, **F1** and **F2:** neutral filters, **A1:** 2 mm aperture diaphragm, **L:** 8 mm focal length lens. (After Ref. [23].)

Variation of the energy density in the sample was made by a reciprocal replacing neutral filters F_1 and F_2. Experimental results for some dye-doped PFNPG samples are shown in Fig 22 and 23.

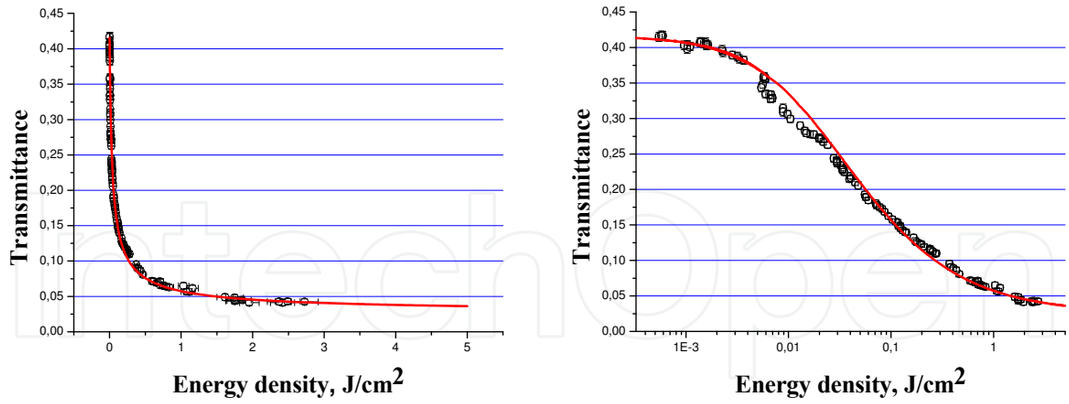

Fig. 22. Transmittance versus laser pulse energy density for PcPb – doped PFNPG composite: linear (left) and log (right) scales. (After Ref. [23].)

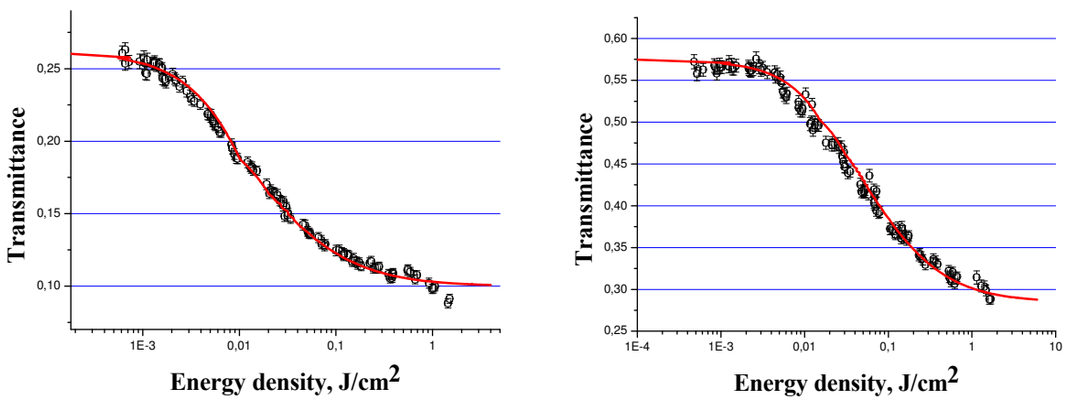

Fig. 23. Transmittance versus laser pulse energy density for PrZn-doped PFNPG (left) and PcZn-doped PFNPG (right) samples. Log scales. (After Ref. [23].)

The following parameters can characterize the transmittance $T(E)$ dependences: a saturation energy density, E_s, a contrast, C_T which is the ratio of the initial transmittance at low intensities to the transmittance at E_s, and a nonlinear absorption initiation energy $E_{th} = (T(0) + T(E_s))/2$ (parameter E_{th} is called somewhere, by mistake, "threshold energy density"). These parameters for some dye-doped PFNPG composite materials are presented in Table 8.

	PcPb	PcZn	PrZn
C_T	10	2.1	2.4
E_{th}, J/m²	580	460	100
E_s, J/m²	19520	7910	1680

Table 8.

5. Conclusions

The data presented in this chapter on the properties of the polymer-filled nanoporous glass showed that this composite is the perspective material of laser optics for making solid-state dye-lasers in the visible and near-IR spectral ranges and a different type of "passive" optical elements: saturable absorbers, radiation power limiters, etc.

To the present, the technology of this material including its impregnation with functional organic compounds (dyes), both "the active" (lasing) and "passive" (controlling radiation amplitude – temporal characteristics) has been developed. The comprehensive studies of structure and optical properties of the material have been carried out and the operation of the optical elements in lasing and controlling modes has been successfully demonstrated.

At the same time, it ought to be pointed out that these studies have been carried out in the laboratory experiments, and further efforts have to be made for improving the technology of the material (to bring it to an industrial level) to make possible the wide practical applications of this new material of laser optics. A relalization of these efforts will lead, as may be expected, to further development of works on dye lasers and laser radiation control elements, and their applications.

6. References

[1] A.M.Dolotov, M.F.Koldunov, N.M.Sitnikov, et al. USSR Patent AC №1814475 (1990).

[2] O.S.Molchanova, Sodium-borate-silicate and porous glasses. Moscow, *Oborongiz*, p. 162, (1961).

[3] N.S.Andreev, O.V.Mazurin, U.A.Poray-Koshits, G.P.Roskova, V.N.Filipovich, Liquation phenomena in glasses. Leningrad, *Nauka*, p. 220, (1974)

[4] O.V.Mazurin, G.P.Roskova, V.I.Averyanov, T.V.Antropova, Two-phase glasses: structure, properties, application. Leningrad, *Nauka*, p. 276 (1991).

[5] G.B.Al'tshiler, E.G.Dul'neva. A.V.Erofeev, et al., Phototropic shutters utilizing micro-porous glass activated by dye molecules. *Quantum Electron*, Vol. 12, p. 1094-1096, (1985)

[6] G.B.Al'tshiler, E.G.Dul'neva, A.V.Erofeev, I.A.Mokienko. Solid-state-liquid passive laser switch – *Pisma in J. Tech. Phys*. Vol. 14, p. 2290 (1988).

[7] G.B.Al'tshiler, E.G.Dulneva, I.K.Meshkovsky, K.I.Krylov. Solid-state active media based on dyes. *J. App. Spectroscopy*, Vol. 36, p. 592, (1982).

[8] S.M.Dolotov, M.F.Koldunov, A.A.Manenkov, et al., Composite material for laser elements based on polymer and microporous glass, *Quantum Electron*, Vol. 22, p. 1060-1062, (1992)

[9] M.F.Koldunov, A.A.Manenkov, N.M.Sitnikov, et al, *Proc. of Laser optics '93*. Russia, St. Peterburg, 1993, Vol.1, p. 246.

[10] M. F. Koldunov, A. A. Manenkov, N. M. Sitnikov, et al, Dye-impregnated polymer-filled porous glass: a new composite material for solid state dye lasers and laser beam control optical elements. *Proc. SPIE* Vol. 2114, p. 101 (1994)

[11] H. R. Aldag, S. M. Dolotov, M. F. Koldunov, et al., Efficient solid state dye lasers based on polymer-filled microporous glass, *Proc. SPIE* Vol. 3929, pp. 133-145 (2000).

[12] H.R.Aldeg, S.M.Dolotov, M.F.Koldunov, et al., Microporous glass – polymer composite as a new material for solid-state dye lasers. I. Material properties. *Quantum Electron*, Vol. 30 (11), pp. 954-958, (2000)

[13] H.R.Aldeg, S.M.Dolotov, M.F.Koldunov, et al., Microporous glass – polymer composite as a new material for solid-state dye lasers. II. Lasing properties, Quantum *Electron*, Vol. 30 (12), pp. 1055-1059, (2000)
[14] J. A. Russell, D. P. Pacheco, H. R. Aldag, S. M. Dolotov, M. F. Koldunov, et al., Beam-quality measurements on solid state dye lasers using nonconfocal unstable resonators. *Proc. SPIE* Vol. 4267, pp. 36-46 (2001)
[15] S.M.Dolotov, M.F.Koldunov, Ya.V.Kravchenko, et al., An efficient solid-state laser based on a nanoporous glass — polymer composite doped with phenalemine dyes emitting in the 600 - 660-nm region. *Quantum Electron*, Vol. 32 (8), pp. 669-674, (2002)
[16] M.F.Koldunov, Ya.V.Kravchenko, A.A.Manenkov, I.L.Pokotilo, Relation between spectral and lasing properties for dyes of different classes. *Quantum Electron*, Vol. 34, pp. 115-119, (2004).
[17] M. F. Koldunov and A. A. Manenkov, Polymer-filled nanoporous glass: a new material for solid-state dye lasers and nonlinear optical elements. *Proc. SPIE* Vol. 6054, pp. 605401-07 (2005)
[18] S. S. Anufrick, M. F. Koldunov, Yu. M. Kuznetsov, A. A. Manenkov, et al., Lasing characteristics of phenolemine 512 and pyrromethene 580 dyes, impregnated to polymer-filled nanoporous glass, at various excitation wavelengths, *Proc. SPIE* Vol. 6054, pp. 60540V-60545V (2005)
[19] A.A.Manenkov, M.F.Koldunov, S.S.Anufrik, New material for laser optics: nanoporous glass polymer composite activated by functional organic compounds. *Proc. of VI International Conf. «Laser physics and optical technology»* Belarus, Grodno, 2006, Vol. 1, pp. 13-17.
[20] S. S. Anufrik, M. I. Ihnatouski, M. F. Koldunov, et al., Optical, structural, and lasing properties of a composite material nanoporous glass filled with an organic dye activated polymer, *Proc. SPIE* Vol. 6735, pp. 67351X-673516X, (2007)
[21] V. Tarkovsky, S. Anufrik, M. Koldunov, and A. Manenkov, The space-angular characteristics of a microsecond solid laser on the basis of a nanoporous glass polymer composite activated with dyes. *Proc. SPIE* Vol. 6731, pp. 673137-673143. (2007)
[22] L.M.Koldunov, M.F.Koldunov, A.V.Petuhov, A.V.Sizuhin, Reversible nonlinear absorption in nanoporous glass polymer composite doped with functional dyes: experiment and background model. *Technical digest*, ICONO/LAT 2010, Russia, Kazan, August 23-26, 2010. ITuQ46
[23] L.M.Koldunov, M.F.Koldunov, A.V.Petuhov, A.V.Sizuhin, Reversible nonlinear absorption in nanoporous glass polymer composite doped with functional dyes: experiment and background model. *Proc. SPIE*. (in press)
[24] L.M.Koldunov, M.F.Koldunov, I.L.Pokotilo, et al., Nonlinear refraction and nonlinear absorption in nanoporous glass composite activated by functional dyes. *Technical digest*, ICONO/LAT 2010, Russia, Kazan, August 23-26, 2010, ITuQ11
[25] L.M.Koldunov, M.F.Koldunov, I.L.Pokotilo. et al, Nonlinear refraction and nonlinear absorption in nanoporous glass composite activated by functional dyes. *Proc. SPIE*. (in press)
[26] K.M.Dumaev, A.A.Manenkov, A.P.Maslukov, et al., Laser radiation interaction with optical polymers – Trudy IOF RAN the USSR, Vol. 33, p. 144, (1991)
[27] S.P.Zhdanov, Physics and chemistry of silicates. Leningrad, *Chemistry*, p. 195 (1987).
[28] W.Vogel, Glaschemie, Leipzig, p. 434, (1979)

[29] T.A.Speranskaj, L.I.Tarutina, Optical properties of polymers. Leningrad, *Chemistry*, p. 136 (1976).
[30] A.P.Babichev, N.A.Babushkin, A.M.Bratkovckii, et al., Fiz. velichiny. Moscow, *Energomashizdat*, p. 1232, (1991).
[31] D.S.Sanditov, G.M.Bartenev, Physical properties of disordered structures. Novosibirsk, *Nauka*, p. 259, (1982)
[32] H.C. van de Hulst. Light scattering by small particles. New York. John Wiley&Sons Inc. London. Chapman&Hall Ltd. p. 536, (1957).
[33] M.Born, E.Wolf, Principle of optics. Pergamon press, Oxford, p. 855, (1964).
[34] I.S.Zeilikovich, A.M. Lyalikov, Holographic methods for regulating the sensitivity of interference measurements for transparent media diagnostics. *Sov. Phys. Usp.* Vol. 34 (1) pp. 74–85 (1991)
[35] C.R.Giuliano, Laser-induced damage to transparent dielectric materials. - *Applied Physics Letters*, 1964, Vol. 5, p. 137-139
[36] A.A.Manenkov, A.M.Prokhorov, Laser-induced damage in solids. *Sov. Phys. Usp*. Vol. 29 pp. 104–122 (1986)
[37] A.A.Manenkov, Fundamental mechanisms of laser-induced damage in optical materials: understanding after a 40-years research. *Proc. SPIE*, Vol. 27132, p. 2-11, (2008)
[38] M.F.Koldunov, A.A.Manenkov, Recent progress in theoretical studies of laser-induced damage (LID) in optical materials: fundamental properties of LID threshold in the wide-pulse-width range from microseconds to femtoseconds. *Proc. SPIE* Vol. 3578, pp. 212-226 (1999)
[39] M.F.Koldunov, A.A.Manenkov, I.L.Pokotilo. Pulse-width dependenct of the laser damage threshold of the transparent dielectric containing the absorbing inclusions. *Bulletin of the Russian Academy of Sciences*. (Physics) Vol. 59, pp. 72-83, (1995).
[40] M.F.Koldunov, A.A.Manenkov, I.L.Pokotilo, Pulse-width and pulse-shape dependencies of laser-induced damage threshold to transparent optical materials. *Proc. SPIE* Vol. 2714, pp. 718-730, (1996)
[41] M.F.Koldunov, A.A.Manenkov, I.L.Pokotilo, Multishot laser-induced damage in optical materials: an analysis of main regularities. *Proc. SPIE* Vol. 3244, pp. 641-649, (1998)
[42] M.F.Koldunov, A.A.Manenkov, I.L.Pokotilo. Multishot laser damage in transparent solids: theory of accumulation effect. *Proc. SPIE* Vol. 2428, pp. 653-667, (1995)
[43] M.F.Koldunov, A.A.Manenkov, I.L.Pokotilo. Theoretical analysis of the accumulation effect in laser damage in transparent dielectrics under repeatad irradiation conditions. *Quantum Electron*, Vol. 22, pp. 674-678. (1995).
[44] H. Ebert, Physikalisches taschenbuch, Frieder, Vieweg&Sohn p. 552, (1957).
[45] M. Sheik-bahae, A.A. Said, T. Wei, et al, Sensitive measurement of optical nonlinearities using a single beam. *IEEE J. of Quantum Electronics*, Vol. 25 (4) pp. 760-769, (1990).
[46] Kamjou Mansour, Daniel Alvarez, Kelly J. Perry, et al., Dynamics of optical limiting in heavy-atom substituted phthalocyanines. *SPIE 1853*, pp, 132-140, (1993).
[47] J. S. Shirk, R.G.S. Pong, et al., Optical limiter using a lead phthalocyanine. *Appl. Phys. Lett* 63, pp. 1880-1882, (1993).
[48] Weijie Su and Thomas M. Cooper , Mark C. Brant. Investigation of Reverse-Saturable Absorption in Brominated Porphyrins. *Chem. Mater*. 10, pp. 1212-1213 (1998).
[49] Kai Dou, Xiaodong Sun, Xiaojun Wang et al. Optical limiting and nonlinear absorption of exited states in metalloporphyrin-doped sol gels. *IEEE Journal of Quantum Electronics*, 35 (7) pp.1004-1013, (1999)

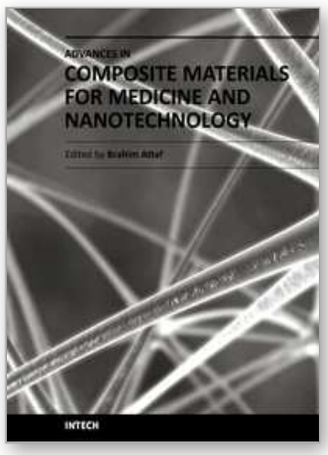

Advances in Composite Materials for Medicine and Nanotechnology

Edited by Dr. Brahim Attaf

ISBN 978-953-307-235-7
Hard cover, 648 pages
Publisher InTech
Published online 01, April, 2011
Published in print edition April, 2011

Due to their good mechanical characteristics in terms of stiffness and strength coupled with mass-saving advantage and other attractive physico-chemical properties, composite materials are successfully used in medicine and nanotechnology fields. To this end, the chapters composing the book have been divided into the following sections: medicine, dental and pharmaceutical applications; nanocomposites for energy efficiency; characterization and fabrication, all of which provide an invaluable overview of this fascinating subject area. The book presents, in addition, some studies carried out in orthopedic and stomatological applications and others aiming to design and produce new devices using the latest advances in nanotechnology. This wide variety of theoretical, numerical and experimental results can help specialists involved in these disciplines to enhance competitiveness and innovation.

How to reference

In order to correctly reference this scholarly work, feel free to copy and paste the following:

Modest Koldunov and Alexander Manenkov (2011). Dye Doped Polymer-Filled Nanoporous Glass - a New Class of Materials for Laser Optics, Advances in Composite Materials for Medicine and Nanotechnology, Dr. Brahim Attaf (Ed.), ISBN: 978-953-307-235-7, InTech, Available from: http://www.intechopen.com/books/advances-in-composite-materials-for-medicine-and-nanotechnology/dye-doped-polymer-filled-nanoporous-glass-a-new-class-of-materials-for-laser-optics

INTECH
open science | open minds

InTech Europe
University Campus STeP Ri
Slavka Krautzeka 83/A
51000 Rijeka, Croatia
Phone: +385 (51) 770 447
Fax: +385 (51) 686 166
www.intechopen.com

InTech China
Unit 405, Office Block, Hotel Equatorial Shanghai
No.65, Yan An Road (West), Shanghai, 200040, China
中国上海市延安西路65号上海国际贵都大饭店办公楼405单元
Phone: +86-21-62489820
Fax: +86-21-62489821

© 2011 The Author(s). Licensee IntechOpen. This chapter is distributed under the terms of the Creative Commons Attribution-NonCommercial-ShareAlike-3.0 License, which permits use, distribution and reproduction for non-commercial purposes, provided the original is properly cited and derivative works building on this content are distributed under the same license.

IntechOpen

IntechOpen